

NEW CrH OPACITIES FOR THE STUDY OF L AND BROWN DWARF ATMOSPHERES

ADAM BURROWS,¹ R. S. RAM,² PETER BERNATH,^{2,3} C. M. SHARP,¹ AND J. A. MILSOM⁴

Received 2002 April 23; accepted 2002 June 10

ABSTRACT

In this paper, we calculate new line lists and opacities for the 12 bands of the $A^6\Sigma^+ - X^6\Sigma^+$ transitions of the CrH molecule. Identified in objects of the new L dwarf spectroscopic class (many of which are brown dwarfs), as well as in sunspots, the CrH molecule plays an important role in the diagnosis of low-temperature atmospheres. As a tentative first application of these opacities, we employ our new theoretical CrH data in an atmospheres code to obtain a CrH/H₂ number ratio for the skin of the L5 dwarf 2MASS J1507038–151648 of $\sim(2-4) \times 10^{-9}$, in rough agreement with chemical equilibrium expectations. Since in previous compilations the oscillator strength was off by more than an order of magnitude, this agreement represents a modest advance. However, in order to fit the CrH abundance in the L dwarf spectral class, silicate clouds need to be incorporated into the model. Given that this subject is still in a primitive stage of development, one should view any spectral model in the L dwarf range as merely tentative. Nevertheless, a necessary first step in L dwarf modeling is a reliable CrH opacity algorithm, and this is what we have here attempted to provide.

Subject headings: astrochemistry — infrared: stars — molecular data — stars: atmospheres — stars: fundamental parameters — stars: low-mass, brown dwarfs

1. INTRODUCTION

The CrH molecule has previously been identified in the spectra of sunspots (Engvold, Wöhl, & Brault 1980) and S-type stars (Lindgren & Olofsson 1980), but recently, CrH bands have been identified in the spectra of very low mass stars and brown dwarfs. In fact, the 1–0 and 0–0 bands of the $A^6\Sigma^+ - X^6\Sigma^+$ transition of CrH are now used as primary markers for the new L dwarf spectral class (Kirkpatrick et al. 1999a, 1999b). Hence, accurate CrH line lists and oscillator strengths are needed to calculate the CrH opacities now used to model the spectral energy distributions of these transitional and substellar objects. The ground $X^6\Sigma^+$ state of CrH is well characterized from far-infrared (Corkery et al. 1991) and mid-infrared (Lipus, Bachem, & Urban 1991) measurements. However, until recently, the same could not be said for the $A^6\Sigma^+$ state.

In this paper, we describe the recent spectroscopy of CrH and the constraining laboratory measurements that now allow us to calculate new opacities due to the $A^6\Sigma^+ - X^6\Sigma^+$ transitions of the CrH molecule. In § 2 we discuss the spectroscopy of the CrH molecule. In § 3 we present the procedures and methods by which the new line lists were generated. In § 4 we show how we calculate CrH opacities at a given temperature/pressure (T/P) point, and in § 5 we present representative opacity plots for CrH at temperatures and pressures characteristic of L and brown dwarf atmospheres. In § 6 we provide and describe a few theoretical spectra generated with the new CrH opacity data and derive an approximate CrH abundance in a representative

L5 dwarf atmosphere. Although the focus of this paper is on the derivation of the new CrH line lists and opacities, we use these exploratory synthetic spectra to speculate on various features of observed L dwarf spectra. We plan to develop our findings in a subsequent paper.

2. SPECTROSCOPY OF CrH

Although the CrH molecule has been known since 1937 (Gaydon & Pearse 1937), its electronic spectra were poorly characterized until 1993, when Ram, Jarman, & Bernath (1993) performed a rotational analysis of the 0–0 band of the $A^6\Sigma^+ - X^6\Sigma^+$ transition and obtained improved rotational constants for the $v' = 0$ vibrational level of the $A^6\Sigma^+$ state. From the observed perturbations in the $A^6\Sigma^+ - X^6\Sigma^+$ 0–0 band, these authors also provided evidence of a low-lying $a^4\Sigma^+$ state near 11,186 cm⁻¹. Recently, the 1–0 and 1–1 bands of the $A^6\Sigma^+ - X^6\Sigma^+$ transitions were remeasured, and an improved set of constants were obtained for the $v' = 1$ vibrational level of the $A^6\Sigma^+$ state (Bauschlicher et al. 2001). In that work, the band origin of the 2–0 band was determined by fitting the band head position using extrapolated rotational constants for the $v' = 2$ level. In the ground state, all of the available data for $v'' = 0, 1,$ and 2, including the hyperfine-free pure rotational transitions and the hyperfine-free vibration-rotation line positions calculated using the constants of Lipus et al. (1991), were used to obtain an improved set of spectroscopic constants for CrH. This work provided a set of much improved equilibrium vibrational and rotational constants for the $A^6\Sigma^+$ state. The new experimental values are in excellent agreement with the results of an extensive set of ab initio calculations (Bauschlicher et al. 2001). However, no experimental measurements are available of the radiative lifetime of the excited $A^6\Sigma^+$ state. These data are needed to compute oscillator strengths used to derive molecular opacities. Bauschlicher et al. (2001) therefore computed the ab initio transition dipole

¹ Department of Astronomy and Steward Observatory, 933 North Cherry Avenue, Room N204, University of Arizona, Tucson, AZ 85721; burrows@jupiter.as.arizona.edu, csharp@as.arizona.edu.

² Department of Chemistry, University of Arizona, Tucson, AZ 85721; rram@u.arizona.edu.

³ Department of Chemistry, University of Waterloo, Waterloo, ON N2L 3G1, Canada; bernath@uwaterloo.ca.

⁴ Department of Physics, 1118 East 4th Street, University of Arizona, Tucson, AZ 85721; milsom@physics.arizona.edu.

moment function for the $A^6\Sigma^+-X^6\Sigma^+$ transition. They also computed the Einstein A -coefficients for many vibrational bands. The estimated accuracy for these computed transition probabilities is 10%–20%. In § 4 we use these Einstein A -coefficients to derive opacities for the CrH molecule as a function of temperature and pressure.

3. THE GENERATION OF THE LINE LISTS FOR THE $A^6\Sigma^+-X^6\Sigma^+$ TRANSITION OF CrH

In order to calculate the molecular opacities of CrH, the ground-state term values for the $v = 0, 1,$ and 2 vibrational levels were calculated up to $J = 39.5$ using the spectroscopic constants reported in the previous paper (Bauschlicher et al. 2001). The term values for the $v = 3$ vibrational level were also calculated using the extrapolated spectroscopic constants of the ground state. The transition wavenumbers for the main branches $R_{11}, R_{22}, R_{33}, R_{44}, R_{55}, R_{66}, P_{11}, P_{22}, P_{33}, P_{44}, P_{55},$ and P_{66} were taken from the available observations over the observed range of J values. For high J lines beyond the range of our observations, the associated wavenumbers were taken from the predictions based on the constants for the ground and excited states. The excited-state term values for the observed bands were calculated by combining the lower state term values with the transition wavenumbers of the observed main branches. The high- J excited-state term values, for which main branches were not observed experimentally, were taken from the predictions based on the spectroscopic constants for the excited states. Accurate excited-state term values are necessary to predict the line positions in the satellite branches, which were not observed in the spectra because of their very weak intensity. The transition wavenumbers for the satellite branches were calculated by simply taking the difference of the excited- and ground-state term values based on the selection rules. In total, the line positions of the 18 allowed satellite branches, namely, $P_{31}, P_{42}, P_{53}, P_{64}, Q_{12}, Q_{21}, Q_{23}, Q_{32}, Q_{34}, Q_{43}, Q_{45}, Q_{54}, Q_{56}, Q_{65}, R_{13}, R_{24}, R_{35},$ and R_{46} , were calculated for the molecular opacity calculation.

The line strengths of various transitions were evaluated by computing values for $A_{v'-v''} \text{HLF} / (2J' + 1)$ in the branches of the different bands. Here the $A_{v'-v''}$ are the Einstein A -coefficient values for the different bands considered (Bauschlicher et al. 2001), and HLF are the Hönl-London factors of the different branches. The Hönl-London factors were derived by M. Dulick of the National Solar Observatory (M. Dulick 2002, private communication), and except for a typographical error, agree with the expressions in Kovacs (1969). The line positions and line strengths were calculated for the 0–0, 0–1, 0–2, 0–3, 1–0, 1–1, 1–2, 1–3, 2–0, 2–1, 2–2, and 2–3 bands of the $A^6\Sigma^+-X^6\Sigma^+$ system of CrH, where by convention, $v'-v''$ ($=\Delta v$) refers to the upper and lower vibrational quantum numbers. For bands involving $v' = 2$, the excited-state constants were obtained from an extrapolation based on the experimental constants for the $v = 0$ and 1 vibrational levels.

We arrange the computed sets of line strengths and line positions for 12 bands of CrH belonging to the $A^6\Sigma^+-X^6\Sigma^+$ electronic system into 12 separate files. Since absorption bands with the same Δv strongly overlap in wavenumber, the computed spectrum has the appearance of six bands for $\Delta v = -3, -2, -1, 0, 1,$ and 2 . Each line list file contains a listing for each line (sorted by branch) with the

values of v' and v'' for the two states, the rotational quantum number J'' of the lower state, and an index indicating if the transition belongs to a $P, Q,$ or R branch.⁵ Thus, the upper rotational quantum number J' , the wavenumber of the transition, the Einstein A -coefficient of the transition, and the excitation energy (term value) in cm^{-1} of the lower state can be found. Both electronic states are sextets, so each rotational level (N quantum number) is split (by coupling with the net electron spin of $5/2$) into six energy levels: $F_1, F_2, F_3, F_4, F_5,$ and F_6 with $J = N + 5/2, N + 3/2, N + 1/2, N - 1/2, N - 3/2,$ and $N - 5/2$, respectively. Indices (1–6) for these spin components are therefore provided for the upper and lower states and are used to label the branches. The e/f parity of the lower state is also provided, although we do not need it for the opacity calculations. A total of $\sim 14,000$ lines (not including isotopes; § 4) are found in the resulting line list. This is ~ 5 times the size of previous CrH compilations but is still considerably smaller than the $\sim 300,000,000$ lines in the current line list for the triatomic molecule H_2O (Partridge & Schwenke 1997).

4. THE CALCULATION OF CrH OPACITIES

In order to calculate spectral models of brown dwarfs and giant planets, opacities are required. However, the computer time and memory necessary to calculate the contribution to the overall opacity of a large number of molecular lines often precludes (but does not render impossible) calculating detailed opacities during a model atmosphere calculation at each temperature and pressure point. Given this, we prefer to precompute the absorption cross section of CrH and other molecules at a large number of temperature (T) and gas pressure (P) points regularly arranged in a table, so that during a model calculation, the cross section of species such as CrH is calculated by interpolation in that table. For each spectroscopically active molecule, a tabulated T/P point has an associated file that contains the monochromatic absorption cross section in $\text{cm}^2 \text{molecule}^{-1}$ calculated at one-wavenumber intervals over a wide, but fixed, spectral range. No averaging is done. The cross section of that molecule at an arbitrary T/P point is obtained by interpolating between the four closest tabulated values of temperature and pressure. Given the abundance of the molecule, its contribution to the total opacity at a general T/P point is then calculated.

Since the Einstein A -coefficient includes all the details of the intrinsic band strength, together with the Franck-Condon and Hönl-London factors, we do not need to consider these quantities separately. Without considering separate isotopic versions of CrH, only the Einstein coefficient, the lower rotational quantum number J'' , the transition wavenumber ($\bar{\nu}$), the term value of the lower state F'' , and the internal partition function Q are required to obtain the frequency-integrated cross section (line strength):

$$S = \frac{1}{8\pi\bar{\nu}^2} A(2J'' + 1) \exp\left(-\frac{F''hc}{kT}\right) \frac{1 - \exp(-hc\bar{\nu}/kT)}{Q}. \quad (1)$$

⁵ These data are now available in electronic form at <http://bernath.uwaterloo.ca/CrH>.

Here F'' is in wavenumbers and the stimulated emission factor is included.

Given the vibrational and rotational constants w_e , $w_e x_e$, B_e , and D_e for the X and A electronic states (Bauschlicher et al. 2001), the vibrational and rotational contributions to the individual partition functions of the X and A states are calculated using asymptotic formulae from Kassel (1933a, 1933b). The total internal partition function is calculated from

$$Q = 6 \left[Q_r'' Q_v'' + Q_r' Q_v' \exp\left(-\frac{T'hc}{kT}\right) \right], \quad (2)$$

where Q_r'' and Q_v'' are, respectively, the rotational and vibrational partition functions of the X state, Q_r' and Q_v' are the corresponding partition functions of the excited A state, T' is the excitation energy of the A state (in wavenumbers), and the factor of 6 accounts for the multiplicity (the electronic contribution to the partition function). There are, in fact, several other states predicted to lie near the $A^6\Sigma^+$ state (Ram et al. 1993; Dai & Balasubramanian 1993), but their contribution to the sum in equation (2) at the temperatures of interest in brown dwarfs is negligible.

We include, along with the most abundant isotope of chromium (^{52}Cr , which makes up 83.8% of chromium), the contributions of ^{50}Cr , ^{53}Cr , and ^{54}Cr , which make up 4.4%, 9.5%, and 2.4%, respectively. Given the reduced mass of the most abundant isotopic form $^{52}\text{Cr}^1\text{H}$ and the reduced mass of any isotopically substituted form of CrH, the vibrational, rotational, and vibration-rotation coupling constants can be found from the corresponding constants for $^{52}\text{Cr}^1\text{H}$ by multiplying by the square root of the reduced mass ratio raised to an appropriate integer power (Herzberg 1950). By identifying the lower and upper levels involved in a given transition, together with the vibrational and rotational quantum numbers, the shifts in the levels can be approximately calculated. Hence, the displacement in the transition wavenumber is obtained for a given isotopic version of CrH.

However, we do not correct for the slightly different partition functions of the isotopic versions, nor do we allow for the small change in the line strengths due to the shift of the lower energy level (hence, its Boltzmann factor). We also ignore the effect of changes in the line frequency on its oscillator strength and the change in the Franck-Condon factors due to the small changes in the wave functions. We think, however, that these effects are very small compared with the shifting of the line positions and the consequent “filling in” of the absorption between the lines of the main isotopomer. Given equation (1) above, the line strength for each isotopic version is obtained by multiplying it by the fractional abundance of that isotope. All 12 files are read, and the lines are calculated by cycling through the data for each of the four isotopes.

Finally, in order to calculate the absorption cross section per molecule on a frequency grid, the integrated line strengths are multiplied by a suitably broadened profile. Our broadening algorithm is an extension of that employed for FeH by R. Freedman (1999, private communication) based on a Lorentzian line shape function. For each line given in an input file, the parameter W_L is given (as provided by R. Freedman), which is the line full width in cm^{-1} at 296 K and 1 atm. At other temperatures and pressures, a scale factor of

$(296 \text{ K}/T)^{w_x} (P_{\text{H}_2}/1 \text{ atm})$ is used, where w_x is 0.7. The value of W_L is generally $\sim 0.045 \text{ cm}^{-1}$.

This whole process is repeated for all four isotopic forms of CrH at all the tabular T/P points. The opacities at a given general T/P point are obtained by interpolation in these files.

5. REPRESENTATIVE CrH OPACITY PLOTS

Using the procedures described in § 4, we have created a program for generating CrH cross sections for the six resulting band sequences with band heads from ~ 0.7 to $\sim 1.4 \mu\text{m}$. Readers can obtain tables generated by this program from the first author. Figure 1 depicts the resulting CrH cross sections for representative pressures and temperatures at which CrH is typically found in substellar atmospheres. Specifically, opacity spectra for T/P pairs of 1500 K/10 bars (*red*), 2000 K/10 bars (*green*), and 2000 K/100 bars (*blue*) are portrayed. The corresponding opacities using the older database for the 0–0 transition of CrH of Ram et al. (1993), as calculated by R. Freedman (1999, private communication), are 2 orders of magnitude weaker. The lion’s share of the difference between the old and the new CrH opacities can be traced to an increase by a factor of ~ 13.5 in the oscillator strength and to a previously inappropriate division by 6, the electronic spin degeneracy factor. The $A-X$ 0–0 band at $\sim 0.86 \mu\text{m}$ (just shortward of the neighboring FeH feature at $\sim 0.87 \mu\text{m}$) and the $A-X$ 0–1 CrH band near $\sim 0.997 \mu\text{m}$ (just longward of the classic Wing-Ford band of FeH) are prominent and, in principle, diagnostic features in measured L dwarf spectra (Kirkpatrick et al. 1999a, 1999b, 2000). Importantly, Kirkpatrick et al. (1999a, 2000) demonstrate that the strengths of these two CrH bands peak near a subtype of L5–L6 and that at later subtypes (which are in principle at lower T_{eff}), they gain ascendancy over the associated FeH features. As is clear from a comparison of the red and green or blue curves, away from the band heads, the CrH opacity is an increasing function of temperature. Furthermore, and as expected, higher pressures result in greater line overlap and hence a smoother opacity spectrum.

Some other molecules that are important opacity sources in the atmospheres of substellar mass objects include H_2O , H_2 , CO , CH_4 , TiO , and VO . To provide the context of the new CrH opacities, we portray in Figure 2 the CrH, H_2O , and VO per molecule cross sections at 1500 K and 10 bars. In atmosphere calculations, the abundances are also germane, but Figure 2 indicates the different wavelength regions for which each of these species is important. As Figure 2 indicates, CrH can be prominent shortward of $1 \mu\text{m}$, particularly after the higher temperature species TiO and VO recede from view.

6. THE INFERRED CrH ABUNDANCE IN AN L DWARF ATMOSPHERE

Theoretically, both CrH and FeH should be important as T_{eff} decreases through 2000 K, reaches the main-sequence edge ($T_{\text{eff}} \sim 1600\text{--}1750 \text{ K}$; Burrows et al. 2001), and dives into the brown dwarf realm. Hence, with T_{eff} for L dwarfs from ~ 2300 to $\sim 1300 \text{ K}$ (a range that straddles the stellar-substellar boundary), CrH should be particularly relevant in their atmospheres (Pavlenko 2001; Kirkpatrick et al. 1999a, 1999b).

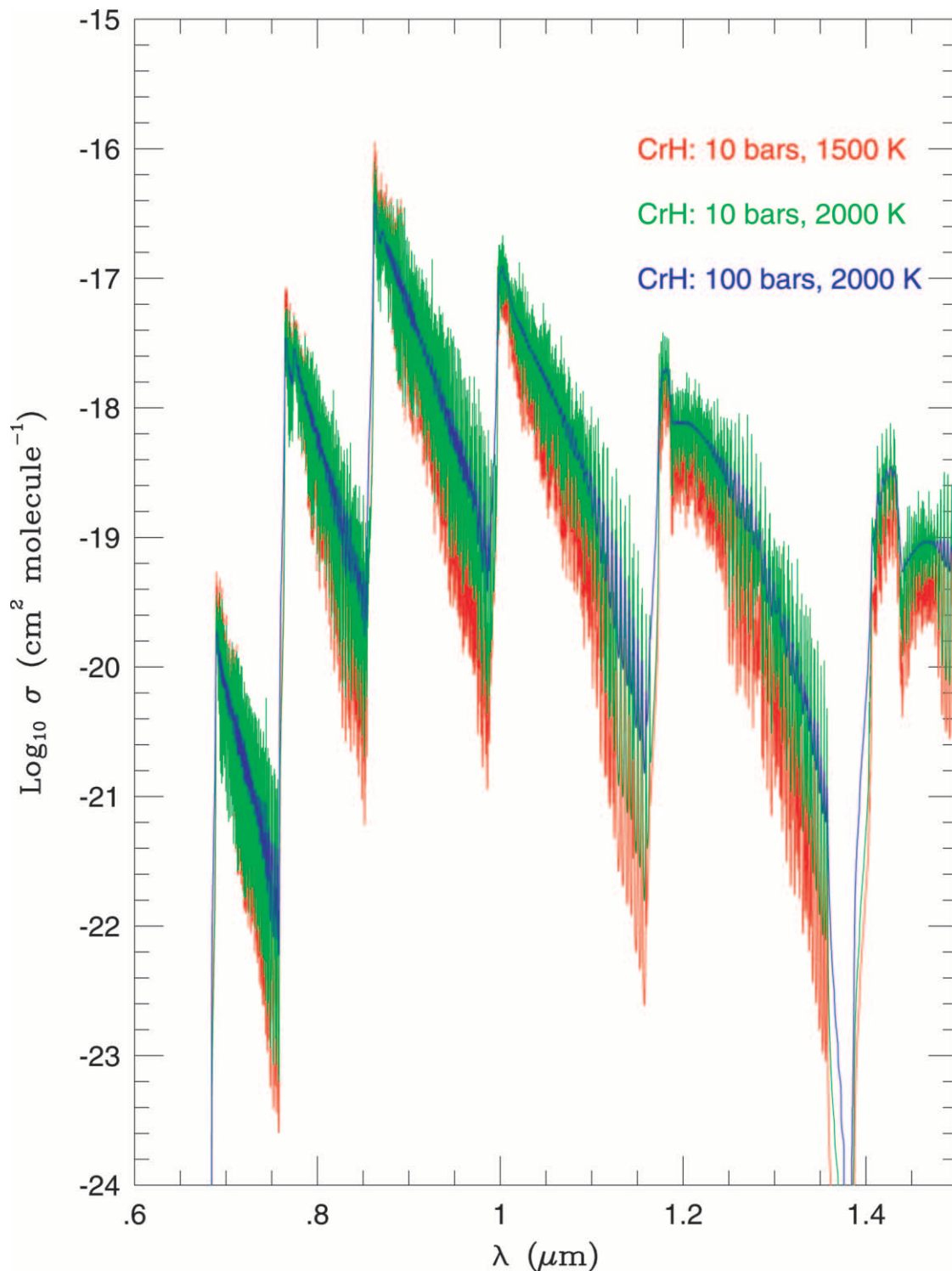


FIG. 1.—Logarithm (base 10) of the absorption cross section of CrH vs. wavelength (in microns) from ~ 0.7 to $1.5 \mu\text{m}$, at various temperatures and pressures. The blue curve at 100 bars and 2000 K depicts the effect of large pressure broadening (when compared with the red curve at 10 bars and 1500 K). A comparison of the green curve (10 bars, 2000 K) with the red curve (10 bars, 1500 K) portrays the effect of increasing temperature. The $A-X 0-0$ band is the strongest and is the third from the left near $\sim 0.9 \mu\text{m}$. As the temperature and pressure decrease, the cross section range in a given band widens and executes larger variation with wavelength.

Chemical equilibrium studies indicate that CrH is expected to survive to lower temperatures in the atmosphere of an L or brown dwarf than FeH, perhaps reaching temperature levels of ~ 1400 – 1600 K, as opposed to ~ 1500 – 2000 K for FeH. However, the actual CrH abundance in an atmosphere will depend not only on CrH

chemistry, but in principle on the effects of rainout, settling, and depletion in the dwarf's gravitational field (Burrows & Sharp 1999; Lodders 1999) and on nonequilibrium dynamics in the dwarf's convective zone. These phenomena can be difficult to model. Fortunately, with better CrH opacities, one can use L dwarf spectra to con-

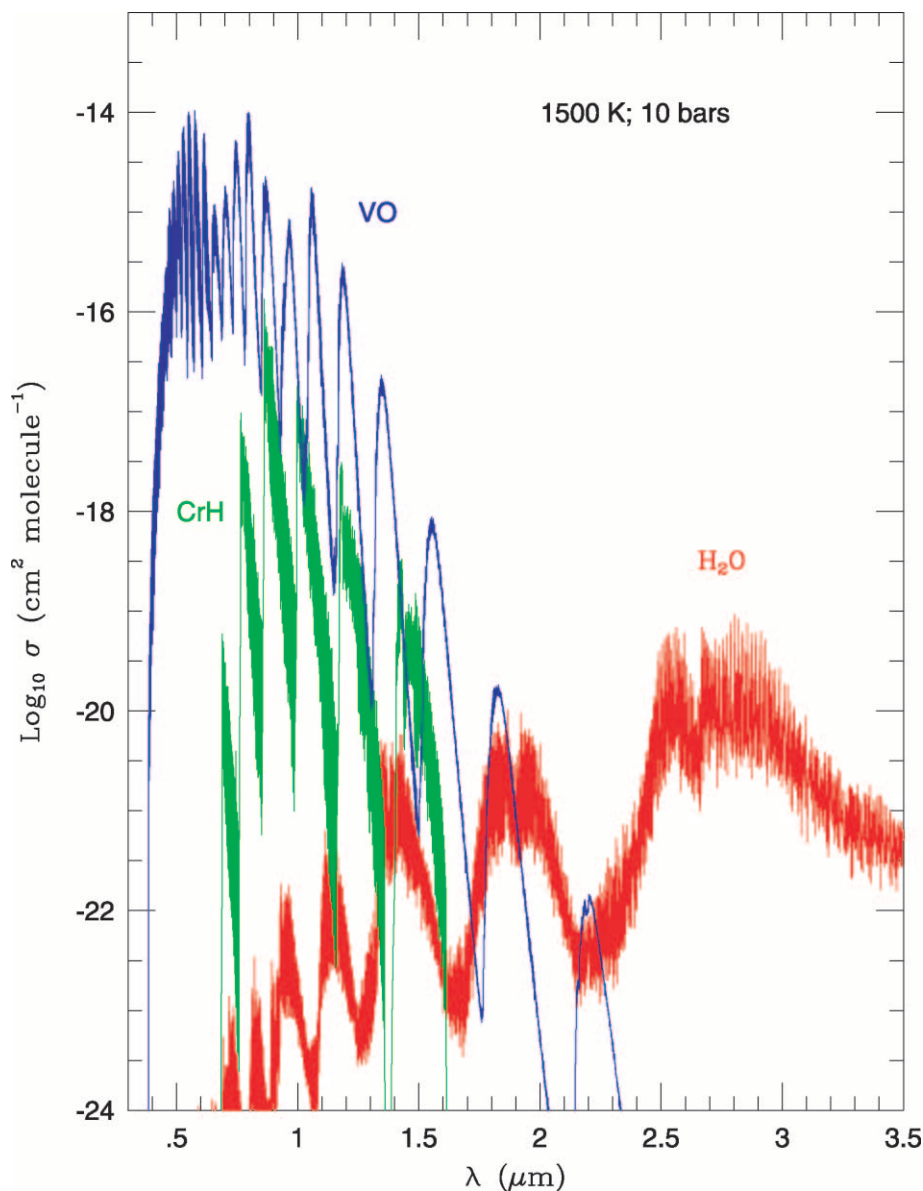


FIG. 2.—Logarithm (base 10) of the absorption cross sections of CrH, H₂O, and VO vs. wavelength (in microns) from ~ 0.3 to $3.5 \mu\text{m}$, at 1500 K and 10 bars. The blue curve with the strong “blue” slope is for VO, a species that is important above ~ 1800 K. The red curve is for H₂O, whose opacity rises toward the near-infrared. The green curve is for CrH (as in Fig. 1), which comes into its own in very cool atmospheres between 2000 and 1400 K.

strain the actual CrH abundances in L dwarf atmospheres. A similar study was recently carried out for the CO molecule by Noll, Geballe, & Marley (1997), who determined that the CO abundance in the upper atmosphere of Gliese 229B is far from its chemical equilibrium value.

In the past, in a reversal of the above philosophy, astronomers have occasionally used stellar spectra to infer the opacity in a spectral band of an exotic but important molecule under nonterrestrial conditions. This was the tradition for TiO and VO in the early days of M dwarf studies (Mould 1976) and has been attempted recently for FeH (Schiavon, Barbuy, & Singh 1997). However, this approach does not allow an independent extraction of the distribution and abundance of the molecule and can lead to very significant errors in the inferred cross sections.

To derive the CrH abundance in a representative L dwarf using the new opacities, we have calculated a few

synthetic L dwarf spectra, using the approach of Burrows et al. (2002). Although the presence of clouds complicates the modeling effort (Burrows et al. 2001), we reach a few preliminary conclusions about both CrH abundances in L dwarfs and the population of L dwarf grains. We modeled clouds that consisted of particles of forsterite (Mg₂SiO₄) with an assumed modal particle size of $50 \mu\text{m}$ (Cooper et al. 2002). The cloud top (for a semi-infinite cloud) was put at an atmospheric temperature level of 1700 K. Above this temperature, all the magnesium was assumed to reside in forsterite. The cloud optical properties were calculated using Mie theory for spherical particles.

In Figure 3 we plot three spectral models from 0.75 to $1.05 \mu\text{m}$ at $T_{\text{eff}} = 1700$ K and for a gravity of $10^{5.5} \text{ cm s}^{-2}$, along with the measured spectrum of the L5 dwarf 2MASS J1507038–151648 (2MASS-1507: *black curve*) (Kirkpatrick et al. 1999b). This L dwarf should be near the main-

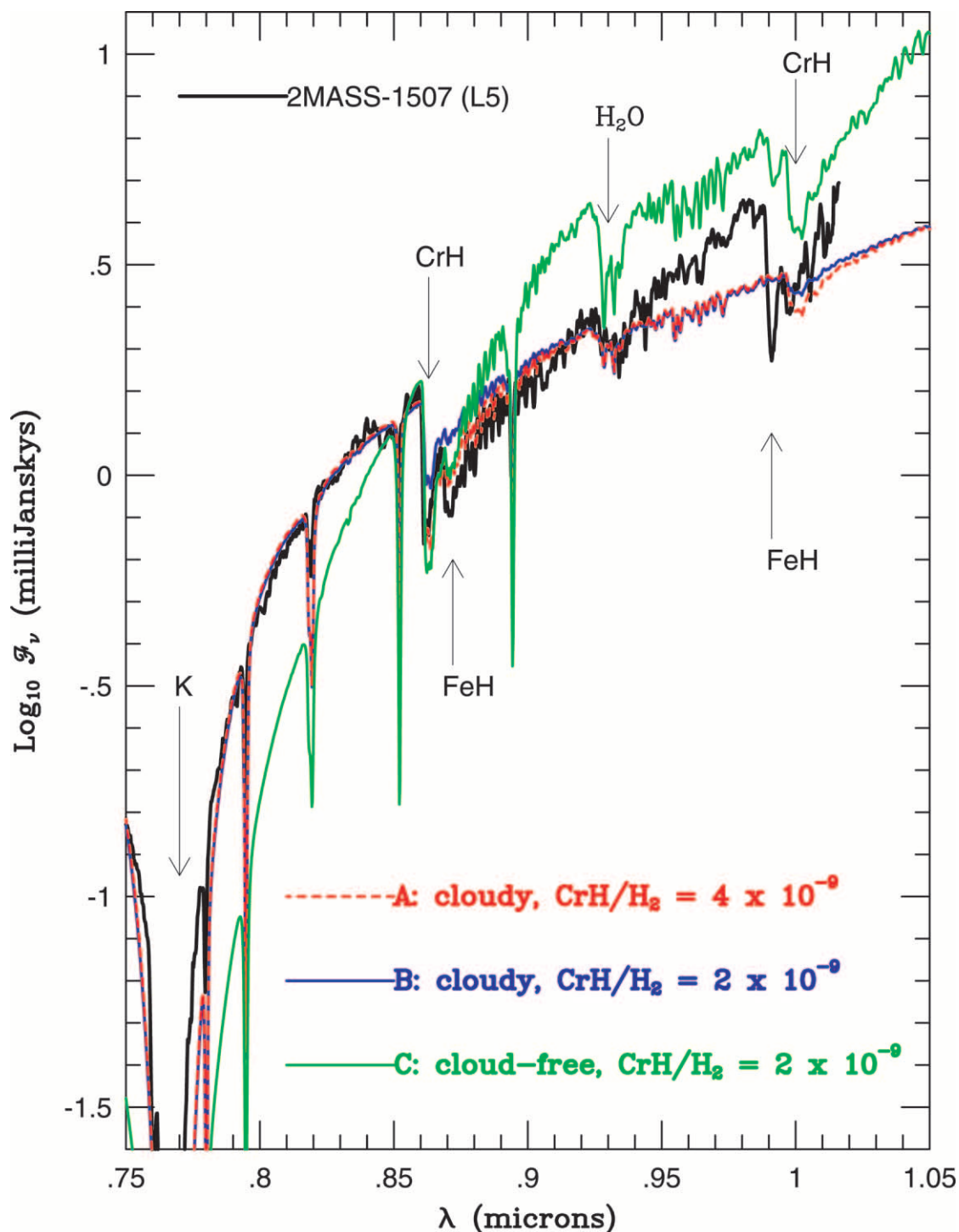


FIG. 3.—Logarithm (base 10) of the absolute flux density \mathcal{F}_ν in millijanskys vs. wavelength (λ) in microns from 0.75 to 1.05 μm for self-consistent theoretical solar-metallicity models of the L5 dwarf 2MASS-1507. Also included are the corresponding data (black line) for 2MASS-1507 from Kirkpatrick et al. (1999a). All models are for $T_{\text{eff}} = 1700$ K and a gravity of $10^{5.5} \text{ cm s}^{-2}$. The dashed red line depicts a model (A) with a forsterite cloud and a CrH/H₂ number abundance ratio of 4×10^{-9} , the blue line depicts a model (B) with a forsterite cloud and a CrH/H₂ number abundance ratio of 2×10^{-9} , and the green line depicts a cloud-free model (C) with a CrH/H₂ number abundance ratio of 2×10^{-9} . Below temperatures of 1400 K, the CrH abundance was set to zero. Indicated with arrows are the positions of the CrH, FeH, H₂O, and K $\lambda 7700$ features in this spectral range. Also prominent are the Cs I $\lambda\lambda 8523, 8946$ lines, the Na I $\lambda 8195$ line, and the Rb I $\lambda\lambda 7802, 7949$ lines. These spectra have been deresolved to an $R(\lambda/\Delta\lambda)$ of 1000.

sequence edge. Clearly seen in the 2MASS-1507 data are the two major CrH bands near 0.86 and 1.0 μm . (Note that the theoretical FeH opacities are currently undergoing a major revision and that we are using for these calculations the old set, now known to be substantially off [P. Bernath et al., in preparation]). Hence, we make no attempt to fit the FeH fea-

tures at ~ 0.87 and $\sim 0.99 \mu\text{m}$, each of which is adjacent to a CrH feature.)

The green curve in Figure 3 is a model (model C on the figure) without grains and has a CrH/H₂ number abundance ratio of 2×10^{-9} above 1400 K. This curve is clearly too steep to explain the spectrum of 2MASS-1507 shortward

of 1 μm . The red and blue curves (models A and B on Fig. 3) include the forsterite cloud with 50 μm particles and have CrH/H₂ abundance ratios of 4×10^{-9} and 2×10^{-9} , respectively. These values seem to bracket the 2MASS-1507 data. Shortward of 0.85 μm , the cloudy models fit much better than the cloud-free model but are too flat longward of 0.95 μm . Presumably, this flatness at longer wavelengths is a consequence of our imperfect cloud model and the assumed wavelength dependence of the real and imaginary indices of refraction of the grains (Scott & Duley 1996). For a given T_{eff} , since clouds suppress flux in the *Z* and *J* bands (not shown), radiation must come out somewhere else. It does so in just the right region shortward of $\sim 0.85 \mu\text{m}$ to compensate for the flux deficit of the cloud-free model there (Fig. 3). Hence, for mid-L spectral subtypes, the combination of K I wing opacity (Burrows, Marley, & Sharp 2000) with our forsterite cloud opacity can approximately account for what is seen shortward of 0.95 μm . Moreover, the cloud decreases the depth of the 0.93 μm water feature (A [red line] or B [blue line] model vs. C [green line] model), in accord with the observations (*black line*). For T dwarfs in the optical (Burrows et al. 2002), the strong effect of clouds is missing, and the corresponding slope is steeper and dominated by the red wing of the 7700 Å feature of K I alone. This slope change is characteristic of the *L* \rightarrow *T* transition. For 2MASS-1507, we are not able to obtain even crude fits in the optical or 2MASS-1507's *J*–*K* color near 1.41 mag (Dahn et al. 2002) without clouds or for clouds with small particles (e.g., ~ 0.1 – $1.0 \mu\text{m}$). Nevertheless, our cloud model is primitive. Fortunately, the inferred CrH abundance is not a strong function of cloud properties, and abundances 3 times higher or lower (not shown) are clearly excluded. We conclude that the CrH/H₂ number ratio in 2MASS-1507 is probably in the $\sim (2\text{--}4) \times 10^{-9}$ range. The Anders & Grevesse (1989) elemental abundance of chromium is $\sim 4.4 \times 10^{-7}$

by number, which results in an atmospheric CrH/Cr number ratio of $\sim (2.3\text{--}4.5) \times 10^{-3}$ above ~ 1400 K, in reasonable agreement with chemical abundance calculations (M. Marley, R. Freedman, & K. Lodders 2002, private communication).

7. CONCLUSIONS

Using the vibrational and rotational constants for the $A^6\Sigma^+$ state of the CrH molecule recently derived by Bauschlicher et al. (2001), we have calculated new line lists and opacities for the 12 bands of its $A^6\Sigma^+ - X^6\Sigma^+$ transitions. The resulting theoretical data are available from the authors. CrH is a defining molecule of the L dwarf spectroscopic class, and accurate opacities as a function of temperature and pressure are necessary for spectral syntheses and to extract CrH abundances for L dwarf atmospheres. In a tentative first step, we use the new theoretical data to obtain such an abundance for the L5 dwarf 2MASS J1507038–151648. The CrH/H₂ number ratio we find is $\sim (2\text{--}4) \times 10^{-9}$, in reasonable agreement with expectations.

This work was supported in part by NASA under grants NAG 5-10760, NAG 5-10629, NAG 5-7499, and NAG 5-7073. Support was also provided by the NASA Laboratory Astrophysics Program and the Natural Sciences and Engineering Research Council of Canada. The authors would like to thank Richard Freedman for exploring with a parallel set of calculations the consequences of the new line lists for the resultant CrH opacities, M. Dulick for providing the expressions for the Hönl-London factors, and David Sudarsky for helping with the calculations of cloud properties. In addition, they would like to thank Ivan Hubeny for consultations on radiative transfer technique. The new CrH line lists are available at <http://bernath.uwaterloo.ca/CrH> and CrH opacity tables in a fixed format can be obtained from the first author at burrows@as.arizona.edu.

REFERENCES

- Anders, E., & Grevesse, N. 1989, *Geochim. Cosmochim. Acta*, 53, 197
 Bauschlicher, C. W., Jr., Ram, R. S., Bernath, P. F., Parsons, C. G., & Galehouse, D. 2001, *J. Chem. Phys.*, 115, 1312
 Burrows, A., Burgasser, A., Kirkpatrick, J. D., Liebert, J., Milsom, J. A., Sudarsky, D., & Hubeny, I. 2002, *ApJ*, 573, 394
 Burrows, A., Hubbard, W. B., Lunine, J. I., & Liebert, J. 2001, *Rev. Mod. Phys.*, 73, 719
 Burrows, A., Marley, M. S., & Sharp, C. M. 2000, *ApJ*, 531, 438
 Burrows, A., & Sharp, C. M. 1999, *ApJ*, 512, 843
 Cooper, C., et al. 2002, *ApJ*, submitted
 Corkery, S. M., Brown, J. M., Beaton, S. P., & Evenson, K. M. 1991, *J. Mol. Spectrosc.*, 149, 257
 Dahn, C. C., et al. 2002, *AJ*, 124, 1170
 Dai, D., & Balasubramanian, K. 1993, *J. Mol. Spectrosc.*, 161, 455
 Engvold, O., Wöhl, H., & Brault, J. W. 1980, *A&AS*, 42, 209
 Gaydon, A. G., & Pearse, R. W. B. 1937, *Nature*, 140, 110
 Herzberg, G. 1950, *Molecular Spectra and Molecular Structure. I. Spectra of Diatomic Molecules* (New York: Van Nostrand)
 Kassel, L. S. 1933a, *Phys. Rev.*, 43, 364
 ———. 1933b, *J. Chem. Phys.*, 1, 576
 Kirkpatrick, J. D., Allard, F., Bida, T., Zuckerman, B., Becklin, E. E., Chabrier, G., & Baraffe, I. 1999a, *ApJ*, 519, 834
 Kirkpatrick, J. D., Reid, I. N., Liebert, J., Gizis, J. E., Burgasser, A. J., Monet, D. G., Dahn, C. C., Nelson, B., & Williams, R. J. 2000, *AJ*, 120, 447
 Kirkpatrick, J. D., et al. 1999b, *ApJ*, 519, 802
 Kovacs, I. 1969, *Rotational Structure in the Spectra of Diatomic Molecules* (London: Hilger)
 Lindgren, B., & Olofsson, G. S. 1980, *A&A*, 84, 300
 Lipus, K., Bachem, E., & Urban, W. 1991, *Mol. Phys.*, 73, 1041
 Lodders, K. 1999, *ApJ*, 519, 793
 Mould, J. 1976, *ApJ*, 207, 535
 Noll, K., Geballe, T. R., & Marley, M. S. 1997, *ApJ*, 489, L87
 Partridge, H., & Schwenke, D. W. 1997, *J. Chem. Phys.*, 106, 4618
 Pavlenko, Ya. V. 2001, *Astron. Rep.*, 45, 144
 Ram, R. S., Jarman, C. N., & Bernath, P. F. 1993, *J. Mol. Spectrosc.*, 161, 445
 Schiavon, R. P., Barbuy, B., & Singh, P. D. 1997, *ApJ*, 484, 499
 Scott, A., & Duley, W. W. 1996, *ApJS*, 105, 401